



HAL
open science

Weak impact of microorganisms on Ca, Mg-bearing silicate weathering

Oleg Pokrovsky, Liudmila Shirokova, Svetlana Zabelina, Guntram Jordan,
Pascale Bénézeth

► **To cite this version:**

Oleg Pokrovsky, Liudmila Shirokova, Svetlana Zabelina, Guntram Jordan, Pascale Bénézeth. Weak impact of microorganisms on Ca, Mg-bearing silicate weathering. *npj Materials Degradation*, 2021, 5 (1), 10.1038/s41529-021-00199-w . hal-03403423

HAL Id: hal-03403423

<https://hal.science/hal-03403423>

Submitted on 26 Oct 2021

HAL is a multi-disciplinary open access archive for the deposit and dissemination of scientific research documents, whether they are published or not. The documents may come from teaching and research institutions in France or abroad, or from public or private research centers.

L'archive ouverte pluridisciplinaire **HAL**, est destinée au dépôt et à la diffusion de documents scientifiques de niveau recherche, publiés ou non, émanant des établissements d'enseignement et de recherche français ou étrangers, des laboratoires publics ou privés.

Weak impact of microorganisms on Ca, Mg-bearing silicate weathering

Oleg S. Pokrovsky^{1,2*}, Liudmila S. Shirokova^{1,3}, Svetlana A. Zabelina³, Guntram Jordan⁴ & Pascale Bénézeth¹

¹*Geosciences and Environment Toulouse, UMR 5563 CNRS, Toulouse, 31400, France*

²*BIO-GEO-CLIM Laboratory, Tomsk State University, Tomsk, 634050, Russia*

³*N. Laverov Federal Center for Integrated Arctic Research of the Ural Branch of the Russian Academy of Sciences, Arkhangelsk, 163000, Russia*

⁴*Department für Geo- und Umweltwissenschaften, Ludwig-Maximilians-Universität, München, Theresienstr, 41, 80333 München, Germany*

*Correspondence and requests for materials should be addressed to O.S.P.
(email: oleg.pokrovsky@get.omp.eu)*

Abstract

Assessment of the microbial impact on mineral dissolution is crucial for a predictive understanding of basic (Ca, Mg-bearing) silicate weathering and the associated CO₂ consumption, bioerosion and CO₂ storage in basaltic rocks. However, there are controversies about the mechanism of microbial effect, which ranges from inhibiting via nil to accelerating. Towards resolving these controversies, we studied diopside interaction with the heterotrophic bacterium *Pseudomonas reactants* and the soil fungus *Chaetomium brasiliense*. Using a mixed-flow reactor, diopside dissolution rates were measured in the presence of live bacteria with and without nutrients. Several grams of bacterial wet biomass per liter produced no sizable effect. Atomic Force Microscopy allowed in-situ characterization of diopside in the presence of bacteria. Colonization by a biofilm-like assemblage was observed in nutrient-rich media. However, extensive production of exopolymeric substances precluded imaging individual cells. In nutrient-free solution, individual cell attachment to the diopside was recognized, but no specific attachment site was identified. Using batch experiments, the effect of live and dead fungus was studied with and without nutrients. Neither case affected considerably the diopside dissolution rates. SEM imaging of reacted grains did not evidence any specific fungus-mineral interaction. The results provide new nano-level insights into the degree to which microorganisms modify silicate dissolution. Taking into account negligible effects of organic ligands on diopside dissolution as reported earlier, we conclude that the microbial effect on Ca-Mg silicates is weak and the acceleration of dissolution of “basic” silicate rocks in the presence of soil biota is solely due to pH decrease in porewaters.

INTRODUCTION

Chemical weathering of basic (Ca- and Mg-bearing) silicates is a primary factor regulating the climate of our planet via a long-term (million year scale) CO₂ uptake from the atmosphere^{1,2}. Both direct biological (enzymatic action of bacteria, fungi, and plant roots) and indirect physico-chemical (soil porewater pH, extracellular organic ligands and biomass degradation products) mechanisms have been identified for

42 chemical weathering of primary silicate minerals in soil environments³⁻⁸. Among the “aqueous” factors,
43 controlling the intensity of this process, solution pH, pCO₂ and organic compounds produced during
44 enzymatic degradation of vegetation litter or the exudates of soil bacteria and plant roots are believed to be
45 the most important⁹. The organic compounds capable to affect mineral dissolution rate include (but are not
46 limited to) extracellular acid and neutral polysaccharides, simple carboxylic acids, uronic acids (galacturonic,
47 guluronic), peptides and aminoacids^{10,11}, as well as various lichen polyphenolic compounds¹².

48 A positive effect of bacteria and organic ligands on aluminosilicate dissolution is incontestable¹³⁻²⁸.
49 Specifically, this effect is related to the capacity of biota to facilitate the Al-O-Si and Fe-O-Si rate-limiting
50 bond breaking, mostly due to strong complexation of bacterially-originated organic moieties with rate-
51 controlling aqueous Al³⁺(aq) cation²⁹, surface >AlOH₂⁺ and >FeOH₂⁺ sites^{30,31}, or Fe³⁺(aq) mobilization in
52 solution³²⁻³⁷ thus preventing passivation of mineral surfaces by newly-formed Fe(III) hydroxides^{38,39}.
53 However, all the above mentioned mechanisms are not likely to operate for Fe- and Al-free, Ca and Mg
54 dominant silicates. In fact, several experimental works performed over the past two decades unambiguously
55 demonstrated the lack of any sizable impact of CO₂ and organic ligands (at otherwise constant pH) on Ca-
56 and Mg-bearing mineral dissolution at typical soil water environments. The reason for this is rather weak
57 complexation of organic ligands with >CaOH₂⁺ and >MgOH₂⁺ surface sites responsible for the rate-
58 controlling Mg-O and Ca-O bond breaking in these minerals⁴⁰⁻⁴⁷. According to these studies, unreasonably
59 high concentrations of naturally-relevant organic ligands (0.01 – 0.1 M) are necessary to significantly
60 enhance or inhibit mineral dissolution. As a result, the effect of extracellular organic products and in general
61 soil biota on the weathering rate of Mg- and Ca-bearing minerals in natural settings is expected to be weak.
62 Further, works with heterotrophic bacteria and basaltic glass⁴⁸, wollastonite⁴⁵ and olivine⁴⁹ demonstrated that
63 even unrealistically high concentration of live biomass (several gram per liter, regardless of the presence of
64 nutrients) are not capable of substantially accelerating the Ca, Mg or Si release rate from the mineral. As a
65 result, despite the dominant paradigm on the importance of microbes in chemical weathering of Ca-Mg-
66 silicates in soil environments, the impact of biota on dissolution rates of these silicates might be lower than
67 generally thought. This, in turn, may require revisiting the current understanding of biotic control on
68 feedbacks in atmospheric CO₂ consumption vs. silicate weathering processes. To resolve these possible
69 contradictions and to extend the previous results to other alkaline-earth bearing minerals (e.g., crystalline
70 mixed calcium and magnesium silicates), we attempted, in the present study, a rigorous measurements of the
71 dissolution rate of the typical basic silicate diopside (CaMgSi₂O₆) in the presence of aquatic and soil
72 microorganisms. For these experiments, we were able to separate the effect of pH from that of bacterial
73 presence using a mixed-flow and batch reactor systems coupled with an in-situ and ex-situ microscopic
74 examination of reacted surfaces.

75 To provide a better understanding of the bacteria–mineral interaction in the context of chemical weathering
76 in soils and CO₂ geological storage, we selected a common soil and underground bacterium, *Pseudomonas*
77 *reactans*. Bacterial strains of the genera *Pseudomonas*, thanks to their relatively easy culturing, have been
78 frequently used as a model organisms in studying mineral weathering in the past^{50,51} and recently^{28,45,52}.
79 Diopside was chosen as a typical model mineral for basic silicates, frequently used as a representative of
80 silicate dissolution at the Earth surface⁵³. Indeed, because hydrolysis of Ca-O and Mg-O bonds is often the
81 rate-limiting step for Ca- and Mg-bearing mineral dissolution⁵⁴, understanding of microorganism interaction
82 with diopside may help to predict the reactivity of other basic silicates in the presence of microbes. In the
83 present study, the experiments were designed in batch and flow-through reactors under constant biomass
84 concentration, in the presence of both live and dead cells in both nutrient-free and nutrient-bearing media.
85 We measured forward far from equilibrium dissolution rates and we microscopically examined reacted
86 surfaces with respect to microorganism attachment, etch pits and corrosion features. Ensemble of obtained
87 results demonstrated rather weak impact of both bacterium and fungus on diopside reactivity, regardless of
88 the presence of nutrients and live status of microorganisms. Moreover, the passivation of mineral surfaces
89 via formation of an exopolysaccharide layer (in case of bacteria) may act as protection mechanism in natural

90 settings. Globally, these new findings challenge the dominant paradigm on dominant biotic control of basic
91 silicates weathering at the Earth surface conditions. This may require revising the quantitative modeling of
92 chemical weathering as main factor of biotically driven long term CO₂ consumption (coupled to Ca and Mg
93 release from silicates). Further, the results call for a need of in-situ assessment of soil porewater pH at high
94 spatial and temporal resolution as a sole factor controlling the rate of Ca, and Mg bearing silicate weathering.

95

96 **RESULTS**

97 **Bacterial Mixed-Flow Reactor (BMFR) with heterotrophic bacterium *P. reactans***

98 In most experiments performed at pH of 6 to 9, stoichiometric release of Si, Ca and Mg was
99 observed. In bacteria-free experiments, diopside dissolution rates decreased by ca. 0.5-1 order of magnitude
100 during the pH decrease from 6 to 9 (Fig. 1, Table 1). Considering certain scatter in the rates obtained in
101 different experiments, the presence of bacteria in either nutrient-free or nutrient-rich media did not exhibit
102 any significant (at $p < 0.05$) effect on Si release rate from diopside, or even led to a decrease of dissolution
103 rates (Fig. 2). In fact, the effect of bacterial presence did not exceed 0.2 log R_{Si} units, whereas the
104 reproducibility of rates measured in individual reactors at otherwise similar aqueous solution composition
105 ranged from 0.1 to 0.3 log R_{Si} units. It can be then concluded that, within the resolution of our experiments,
106 the impact of bacteria on diopside Si dissolution rate could not be quantified or it was below 0.2 log R unit.
107 Furthermore, there was a net inhibiting effect of bacteria on Ca and Mg release rate from diopside in nutrient
108 solution at pH = 6.1 (Fig. 2 A). In more alkaline solutions (pH = 8.5 to 9.0), the presence of bacteria (with or
109 without nutrients) did not considerably (> 0.2 log R unit) impact the release rate of Si, Ca and Mg (Fig. 2 B).

110 The 2nd remarkable result of BMFR experiments is that live bacteria with (D2-2, D2-3, D4-2, D4-3)
111 and without (D1-2, D1-3, D3-2, D3-3) nutrients exhibited a negligible effect of biomass concentration
112 (between 0.54 and 3.85 g_{wet}/L) on Mg, Ca and Si release rates because there was no substantial (> 0.2 log R
113 unit) change in rate during biomass increase by a factor of 7 (Table 1).

114 The 3rd important observation is that there was a significant, by a factor of 3 to 5, decrease in Ca,
115 Mg, Si concentrations and release rates between the beginning (exp. D1-1, D2-1, D3-1 and D4-1) and the
116 end of bacteria-free experiments (exp. D1-4, D2-4, D3-4 and D4-4). This is illustrated in Fig. S1, where the
117 Si concentration in the outlet solution corresponding to the sequence of inlet solutions “bacteria-free 0.1 M
118 NaCl → 0.54 g_{wet}/L bacteria → 3.85 g_{wet}/L bacteria → bacteria-free 0.1 M NaCl”, at a constant flow rate,
119 demonstrated a 3- to 5-fold decrease between the initial and the final bacteria-free experiment. Such a
120 decrease could be related to passivation of mineral surface by bacterial cells and their exometabolites as
121 evidenced from in-situ microscopic observations (see section on the AFM observations below).

122

123 **Calcium, magnesium and silica release rate in batch reactor in the presence of fungus**

124 Results of Ca, Mg and Si release from diopside in 0.1 M NaCl and in nutrient media in the presence
125 of live and dead *Chaetomium brasiliense* demonstrated that concentrations of all mineral constituents
126 increase quasi-linearly with time in all types of experiments (illustrated for Si in Fig. S2 of the Supplement).
127 The linear regression coefficients varied from 0.9 to 0.99 for Si and from 0.8 to 0.95 for Ca and Mg. The pH
128 remained generally constant (± 0.2 unit) or slightly increased (within 0.2 – 0.3 units) over the 19 days of
129 exposure. Taking into account that 1) all solutions are strongly undersaturated with respect to diopside, all
130 other possible Ca and Mg silicates and amorphous silica and 2) there is no effect of aqueous Ca, Mg and Si
131 concentration on diopside forward dissolution rates in neutral solution^{41,55,56}, one can quantify the far-from
132 equilibrium dissolution rates for each individual experiment using the following equation which can be
133 applied over the whole duration of the experiment:

134

$$R = (d[Ca, Mg, Si/2]_{tot} / dt) / s \quad (2)$$

135 where t (s) designates the elapsed time, $[Ca, Mg, Si]_{tot}$ (mol/L) stands for the concentration of calcium,
136 magnesium or silica released from the solid, and s (cm²/L) is the powder B.E.T. surface area. Results are
137 listed in Table 2. The uncertainties on these rates stem from duplicate experiments and range between ± 10
138 and 30%. The rates measured in the presence of dead or live fungi generally agree (within ± 0.2 log units)
139 with those of abiotic and biotic experiments in mixed-flow reactor (Fig. 1). The Si release rates were a factor
140 of 1.5 higher in experiments with live fungus (with or without nutrients) compared to experiments with dead
141 fungus (Fig. 3). However, there was no difference in Mg release rates between different treatments, whereas
142 the Ca release rate, although more variable among replicates, exhibited a maximum in nutrient-free
143 experiments with live fungus (Fig. 3).

144

145 **AFM observation of diopside in the presence of bacteria**

146 Freshly reacted diopside surfaces (2-5 h in sterile NaCl solution) largely preserved their cleavage
147 plane morphology (Fig. 4 A). Occasionally some etch pits and local surface roughness was observable (Fig.
148 4 B). After 36 h reaction in bacteria-free nutrient solution, rounding of edges occurred (Fig. 4 C). After 1 to 2
149 days of reaction with nutrient solution at pH = 8.5 or 6.5, we have observed a strong colonization of diopside
150 surfaces by a biofilm-like bacterial assemblage (Fig. 4 D). This EPS coverage included individual elongated
151 spheres and generally convex forms, less than 0.5 μm in longest axis, although their size distribution was not
152 uniform (Figs. 4 D, E, F). Groups of objects occasionally exhibited a distinct internally preferred orientation,
153 which was, however, quite variable within a relatively small area ($\sim 50 \mu\text{m}^2$). The obtained images are
154 consistent with earlier reported bacterial extracellular polymeric substances (EPS) via AFM^{57,58}. Extensive
155 production of exopolymeric substances precluded imaging of individual bacterial cells within this thick
156 biofilm coverage. In contrast, mineral interaction with bacteria in nutrient-free neutral electrolyte allowed
157 recognizing individual cells attached to the diopside surface (Fig. 4 G); however, no site of preferential
158 interactions such as steps or edges could be identified.

159

160 **SEM imaging of diopside reacted with fungus**

161 The diopside grains reacted with dead fungus in 0.1 M NaCl demonstrated sharp borders and no
162 clear dissolution features (Fig. 5 A). After reaction with live fungus in nutrient-free media, there was an
163 appearance of specific dissolution features such as etching and rounding of edges (Fig. 5 B). The rounded
164 edges were also observed in experiments with live fungus; these features were distinctly different from
165 cleavage (Fig. 5 C). The diopside crystals were also imaged in the presence of fungal mycelium: the hyphae
166 were strongly attached to the grain surfaces and not lost during sample preparation for SEM (Fig. 5 D). Some
167 grains appeared significantly ($> 50\%$) covered by or even embedded into network of fungal hyphae. There
168 were no distinct sites of hyphae location at the diopside surface and overall, the interaction appeared to be
169 quite inert, non-specific and site-indifferent. With increasing the resolution, some organic spherical entities,
170 2 to 3 μm in diameter, were identified at the extremities of the hyphae (Fig. 5 D).

171

172 **DISCUSSION**

173 **Weak (non-measurable) impact of bacterium and fungus on Ca, Mg and Si release rate from diopside**

174 Biologically accelerated weathering of silicates is thought to be controlled by microbial production
175 of extracellular enzymes, chelates, simple and complex organic acids and exopolysaccharides^{9,24,59,60,61}.
176 However, there are serious controversies, whether such an effect is largely direct (metabolically-driven
177 nutrient mobilization and specific ligand production) or indirect (passive pH lowering and cation
178 complexation via EPS excretion), given that it is largely dependent on the nature of mineral and the identity

179 of microorganism^{22,62-67}. Furthermore, considering basic silicates, some studies reported nil or inhibiting
180 effect of bacteria on olivine^{49,68,69} or wollastonite⁴⁵ dissolution, whereas other claimed strong accelerating
181 effect of fungi on olivine^{38,39,70}. However, in the latter works, all the effects of microorganisms were limited
182 to their ability to sequester rate-inhibiting Fe(III) thus preventing the slowdown of dissolution, rather than
183 directly promoting the breaking of structural bonds in the mineral lattice. Overall, in contrast to large number
184 of works on microbial impact on aluminosilicate dissolution⁷¹⁻⁷⁹, the interaction of aquatic microorganisms and
185 relevant organic ligands with Ca or Mg-bearing silicates remained insufficiently characterized.

186 In the present study, the global rate uncertainty in the studied pH range (6 to 9) was between 20 and
187 50%. This uncertainty stems from both the pH variation ($\pm 0.2-0.3$ units) during the course of an experiment
188 and the reproducibility of steady state concentrations of diopside constituents in mixed-flow reactors with
189 bacteria-free systems or among duplicates in batch reactors with dead fungus ($\pm 20\%$). Therefore, we
190 conclude that the difference between abiotic (bacteria-free or dead cells) and live bacteria experiments is
191 within the experimental uncertainty. As such, the effect of selected live microorganisms on Ca, Mg and Si
192 release rate from diopside is not significant, or cannot be resolved using the experimental design employed in
193 the present study.

194 In this regard, the present result corroborates the former works of our group which demonstrated
195 weak inhibiting or negligible impact of cultivable heterotrophic bacteria *P. aureofaciens* on wollastonite⁴⁵
196 and *P. reactans* on basaltic glass⁴⁸ and olivine⁴⁹, in agreement with other studies^{28,64,68}. The broad meaning of
197 these results is that microbial impact on basic silicate mineral dissolution is limited by *i*) pH decrease, thus
198 accelerating proton-promoted dissolution, which is relevant to all basic silicates; *ii*) release of Fe(III)-
199 complexing organic ligands including siderophores. The latter is pertinent solely to minerals whose
200 dissolution is limited by Fe(OH)₃ passivation of the surface. In all other cases of microbially-affected basic
201 silicate dissolution, the concentrations of excreted organic ligands are not sufficient to sizably complex Mg
202 and Ca at the surface or in the aqueous solution which is necessary for breaking of rate-controlling Mg-O or
203 Ca-O bonds at the mineral surface. For example, gluconic acid and its derivatives are believed to be the main
204 exometabolite of heterotrophic bacteria that use glucose as substrate^{23,51}. Gluconic acid can favor olivine
205 dissolution in neutral waters⁴⁹; however, this effect occurs at concentrations > 1 mM, totally irrelevant to
206 natural environments. Another example comes from a concerted study of ~40 various ligand impact on
207 wollastonite dissolution⁴⁵. These authors calculated, based on results in mixed-flow reactors, the threshold
208 concentrations of ligands necessary to triple the rates of wollastonite at pH around 7. For most ligands, very
209 high concentration (2 to 3 orders of magnitude higher than those encountered in natural settings) were
210 necessary to appreciably affect the rates. Finally, Golubev and Pokrovsky (2006)⁴¹ demonstrated that very
211 high concentrations (0.01-0.1 M) of organic ligands originated from enzymatic degradation of organic matter
212 or bacterial metabolic activity, are necessary to appreciably affect diopside dissolution. Considering these
213 results and by analogy with olivine and wollastonite, we hypothesize that possible impact of studied
214 heterotrophic bacteria on the diopside dissolution via gluconic acid or other soluble exometabolite
215 production is not detectable due to insufficient concentration of this acid generated via metabolism of *P.*
216 *reactans* in experimental reactors.

217 218 **Mechanisms of diopside interaction with microbial cells and natural implications.**

219 Reactive surfaces in both bacterial and fungal experiments demonstrated lack of specific sites of
220 dissolution, etch pit formation, surface amorphisation or new mineral occurrences. Rather, our in-situ (AFM)
221 and ex-situ (SEM) microscopic observations suggested “passivation” of reacted surfaces by microbial
222 metabolic products. We therefore hypothesize that the biofilm coverage either limited aqueous solution
223 contact with mineral surface or merely did not produce sufficient amount of organic ligands capable to
224 impact the diopside dissolution.

225 Microbial biofilm formation, dominated by exopolysaccharides (EPS), is known to protect the
226 mineral surface from interaction with bulk fluid^{59,63,64,80} thus inhibiting overall dissolution rate^{4,7,10,11,52,81,82}. In

227 the present experiments with diopside, the biofilm formation was also evidenced from indirect assessment of
228 dissolution rate: the rates decreased by a factor of 2 to 3 after ~500 h treatment with bacteria; this decrease
229 persisted even after changing back the inlet solution to sterile bacteria-free background electrolyte (see Fig.
230 S1). Noteworthy that such an irreversible rate decrease was also observed after reaction with live bacteria in
231 nutrient-free media and suggested substantial and long-lasting interaction of live *P. reactans* with diopside
232 surface in both neutral (pH = 6) and slightly alkaline (pH = 9) solutions.

233 As a result of lack of measurable rate increase in the presence of either bacteria or fungus in this
234 range of pH, nutrient and biomass concentration, we suggest, in agreement with previous studies, that,
235 regardless of nutrient regime, biomass concentration and vital status of microorganism, solely the solution
236 pH can act as the main governing factor of mineral dissolution in the presence of aquatic microorganisms.
237 Therefore, implementation of mineral–microorganism interaction in chemical weathering codes requires
238 solely the information on porewater solution chemistry that can be directly assessed from macroscopic
239 measurements of interstitial soil solutions.

240 Moreover, extremely high concentrations of organic ligands, necessary to affect the rates of basic
241 silicate dissolution in laboratory experiments^{41,45,49}, together with high bacterial and fungi concentrations,
242 comparable with those used in the present study, can be encountered exclusively in surface (litter) soil
243 horizons, and unlikely to ever occur in deep (mineral) soil horizons. Exceptions are specific
244 microenvironments around fungal hyphae, or near decaying organic matter. For example, a strong
245 acidification was reported with hyphae bound to the biotite surface⁸³. To quantify these effects on a broader
246 scale, high-resolution in-situ quantitative analysis of chemical composition of solution, bacteria and organic
247 ligand concentration in soil pore water microenvironments are needed.

248 For more general natural implications of the obtained results, we consider below all Ca, Mg-bearing
249 ‘basic’ silicates including Ca aluminosilicates. Several lines of evidences allow us to suggest rather weak
250 effect of dissolved organics on (Ca, Mg, Al)-bearing silicate dissolution in natural settings. First, the
251 concentration range of various carboxylic ligands (oxalic, citric, malonic, succinic, lactic, formic, acetic),
252 detected in soil solutions, spans from 10^{-6} to 10^{-4} M^{84,85}. Laboratory experiments suggest that these
253 concentrations are still not sufficient to appreciably affect feldspars dissolution rates. Second, the effect of
254 organic ligands on Al release and thus on overall dissolution rates of feldspars and basaltic glass is absent or
255 becomes negligible at $\text{pH} \geq 7$ ^{29,86}. The pH of rivers and streams draining ‘basic’ silicate rocks is between 7
256 and 8⁸⁷⁻⁸⁹ whereas the pH of soil solutions in organic rich soils typically ranges from 4 to 7⁹⁰. However,
257 surficial acid- and organic-rich soil horizons rarely contain primary silicates, whereas in deep (C) soil
258 horizons, the interstitial soil solution pH is always above 7 (see ref. 88). At these conditions, the effect of
259 organic ligands on Ca, Mg, Al and Si release rate from primary silicates should be negligible which
260 corroborates the conclusion of Drever (1994)⁹¹ that vegetation should cause an increase in weathering rate
261 through the pH effect only where the pH is below 4-5. As a results, the sole effect of soil organics on both
262 acidic and felsic rock weathering seems to be in decreasing the aqueous activity of Al^{3+} thus preventing
263 formation of secondary minerals without significant modification of Ca and Mg ions release.

264 It has been widely argued that the presence of soluble minerals in trace amounts in the rocks (i.e.,
265 carbonates^{92,93}; phosphates⁹⁴ may strongly affect the intensity of chemical weathering and export fluxes of
266 major ions. The effect of biological activity in this case is expected to be solely due to pH decrease in the
267 vicinity of microorganisms or plant roots. Indeed, the data for dolomite⁴², calcite and magnesite^{44,46},
268 brucite⁴³, and calcite⁴⁷ dissolution in the presence of various organics demonstrate a negligible effect of
269 organic ligands on Ca and Mg release from carbonates and oxides at environmentally-relevant conditions.
270 The effect of soil and atmospheric pCO_2 is always considered to be an important factor accelerating rock
271 weathering at the Earth surface. In this regard, we would like to underline that this effect stems solely from
272 the decrease of soil solution pH since there is no chemical effect of $\text{CO}_2(\text{aq})$ or dissolved H_2CO_3 molecules
273 on the main rock-forming silicates dissolution rate⁵⁶, and in neutral and alkaline solutions the pCO_2 effect
274 becomes even inhibiting⁹⁵.

275

276 CONCLUDING REMARKS

277 Overall, this work allows a better understanding of microbially-affected basic silicate dissolution and
278 provides new microscopic insights for quantifying the degree to which the heterotrophic bacteria and fungi
279 are capable of modifying the dissolution rate of rock-forming silicates. Using bacterial-mixed flow and batch
280 reactors combined with in-situ atomic force microscopy of bacteria-diopside surfaces and experiments on
281 diopside dissolution in the presence of fungus combined with microscopic examination of reacted surfaces,
282 we demonstrated a rather weak impact of microorganisms on Ca, Mg and Si release rate. Regardless of the
283 presence or absence of nutrients, in a wide range of pH (from 6 to 9) and despite very high biomass
284 concentration (up to 4-5 g_{wet}/L), the rates were not considerably affected by microbial presence. Moreover,
285 there was a detectable (ca. by a factor of 3) decrease in reactivity of diopside after its prolonged contact with
286 live heterotrophic bacteria. This ‘passivation’ of the mineral surface was evidenced by extensive production
287 of exopolymeric substances yielding a biofilm-like coverage already after 1-2 days of interaction in nutrient-
288 rich media. Despite tight contact between fungus and diopside surfaces, no site of preferential interactions
289 such as steps, kinks or edges, etch pits or surface amorphisation was detected. The obtained results are fully
290 consistent with large body of evidences that any possible microbially produced organic ligands at
291 concentrations relevant to live biotic systems or natural settings are not capable of noticeably impacting the
292 reactivity of Mg-O and Ca-O sites on diopside surface. As such, this work challenges the dominant paradigm
293 of an overwhelming role of biota on silicate mineral weathering in soils. At the same time, it is in line with a
294 controversial opinion of Sverdrup (2009)⁹⁶ that physical and chemical conditions of forest soils do not allow
295 any significant direct surface actions on minerals by microorganisms or tree roots. While we do not contest
296 the importance of microbial organic matter in Fe and Al complexation and mobilization from silicate
297 structure, the role of biota on basic (Ca and Mg) silicates, playing a pivotal role in atmospheric CO₂
298 sequestration via chemical weathering, may be much lower than traditionally thought. In fact, only drastic
299 pH decrease (i.e., over several pH units), probably occurring in the microniches adjacent to plant roots, is
300 capable of sizably (> a factor of 2 to 3) increase mineral dissolution rate. It is not excluded however that this
301 promoting effect will be partially attenuated due to biofilm formation and passivation of silicate surfaces by
302 microbial cells. Detecting such ‘active’ or ‘passive’ microniches within the complex plant-microbe-mineral
303 systems and more importantly, characterizing chemical environment of the fluids with spatial resolution on
304 the level of μm to mm may turn out to be a bottleneck for quantitative mechanistic modeling of chemical
305 weathering. Currently, these gradients are not taken into account even in most sophisticated modeling
306 approaches^{97,98}. Further experimental and field studies are thus needed to answer the question whether a
307 quantitative modelling of basic silicate mineral weathering and related CO₂ consumption require an explicit
308 prediction for microbial activity or it can be merely approximated by the pH of bulk soil porewaters.

309

310 MATERIALS AND METHODS

311 Mineral, bacterial and fungal culture

312 Natural diopside (Ca_{0.99}Mg_{0.98}Fe_{0.02}Cr_{0.01}Si₂O₆) crystals characterized in previous works^{41,56} were
313 used in this study. Ultrasonically-cleaned 100 to 200 μm size fraction having a specific surface area of 1045
314 ± 50 cm²/g was selected for dissolution rate measurements.

315 *Pseudomonas reactans* is a common rod-shape groundwater and soil bacteria averaging 2 μm in size
316 (see further description in ref. 48, 49). For experiments, cells were first cultured to a stationary stage on a
317 shaker at 25°C in the darkness using 10% nutrient broth with the following composition: 0.1 g/L glucose, 1.5
318 g/L peptone, 0.6 g/L NaCl and 0.3 g/L yeast extract. Cells were allowed starving for 2 days in nutrient-free
319 media, prior the macroscopic dissolution and microscopic (AFM) experiments.

320 Active bacteria number counts (colony forming-units, CFU/mL) were performed using Petri dish
321 inoculation on a nutrient agar (0.1, 0.2, and 0.5 mL of sampled solution in three replicates) in a laminar hood

322 box. Inoculation of blanks was routinely performed to assure the absence of external contamination. The
323 biomass of live bacteria suspensions was also quantified by measuring wet (after it was centrifuged 15 min at
324 10,000 rpm) and freeze-dried weights in duplicates. Before the experiments, cells were rinsed twice in either
325 the appropriate fresh culture media or a sterile 0.1 M NaCl solution using centrifugation with ~ 500 mL of
326 solution for 1 g of wet biomass, to remove adsorbed metals and cell exudates from the surface. The
327 conversion ratio wet/freeze-dried weight of *P. reactans* was equal to 8.4 ± 0.5 . The conversion factor of
328 optical density (600 nm, 10 mm path) and wet biomass (g_{wet}/L) to the cell number (CFU/mL) was equal to
329 $(5 \pm 1) \times 10^8$ and $(8.0 \pm 1.5) \times 10^7$, respectively as determined by triplicate measurements. Typical live biomass
330 concentration during experiments was 0.54 and 3.85 g_{wet}/L.

331 Experiments on fungus were performed with *Chaetomium brasiliense*, belonging to the largest genus
332 of saprophytic ascomycetes, inhabiting soils worldwide. The environmental habitats of genus *Chaetomium*
333 include deserts, salterns, agricultural, mangrove, living plants and animals, air, decayed wood and stones⁹⁹.
334 *Chaetomium brasiliense* Bat. Et Pontual 1948, stumm F-3649 was obtained from All-Russian Collection of
335 Microorganisms - VKM (<http://www.vkm.ru/Collections.htm>). Fungal biomass was produced on liquid
336 Czapek medium (3 g/L NaNO₃, 1 g/L K₂HPO₄, 0.5 g/L KCl; 0.5 g/L MgSO₄×7H₂O, 0.01 g/L FeSO₄×7H₂O,
337 30 g/L saccharose at pH = 6.0). The biomass was centrifuged at 5000 rpm during 15 min, rinsed 4 times in
338 0.1 M NaCl and allowed starving during 2 days in 0.1 M NaCl prior the experiment. Dead (heat-killed) cells
339 were produced via autoclaving 1 h at 132°C the freshly grown fungal biomass followed by thorough rinsing
340 in sterile 0.1 M NaCl. Cell concentration in the sample was analyzed by measuring optical density (OD) at
341 580 nm using a spectrophotometer, with the culture medium used as a reference. Diopside dissolution
342 experiments were performed in duplicates, in 0.1 M NaCl with dead biomass, and live biomass with and
343 without nutrients.
344

345 **Bacterial mixed-flow reactor**

346 The Bacterial Mixed-Flow Reactor (BMFR) system used in this work was similar to the one used for
347 basaltic glass dissolution in the presence of bacteria⁴⁸. The Teflon-made 25 mL reactor with a suspended
348 Teflon-coated stirbar, immersed in a water bath at 25 ± 0.5 °C, was fitted with 20 µm poresize Magna
349 Millipore Nylon outlet filters (45 mm diameter) to allow bacteria to pass while retaining the 100-200 µm
350 mineral powder in the reactor. This system therefore maintained a constant biomass concentration in the
351 reactor, equal to that of the inlet fluid. The input fluids were kept in 1L polypropylene bottles closed with
352 Biosilico® ventilated caps. These fluids were stirred continuously during the experiments and were changed
353 typically each 7 days. This allowed maintenance of a constant and stable stationary phase bacterial culture in
354 the bacteria-bearing inlet fluid. Bacteria concentration was verified by periodical sampling of inlet and outlet
355 fluids for cell optical density (total biomass) and live cell numbers (via agar plate counting). Prior to each
356 experiment, all reactor system parts, including tubing, were sterilized at 130°C for 30 min and rinsed with
357 sterile MilliQ water.

358 Steady-state dissolution rates (R_i , mol/cm²/s) were computed from measured solution composition
359 using:

$$360 \quad R_i = -q \cdot 1/n \cdot \Delta[i(\text{aq})]_{\text{tot}} / s \quad (1)$$

361 where q (L/s) designates the fluid flow rate, $\Delta[i(\text{aq})]_{\text{tot}}$ (mol/L) stands for the difference between the input
362 and output solution concentration of i -th element, n is the stoichiometric coefficient of i -th element in
363 diopside formula equal to 2, 1, and 1 for Si, Mg and Ca, respectively, and s (cm²) refers to the total mineral
364 surface area present in the reactor. The surface area used to calculate the rates was that measured on the fresh
365 (unreacted) diopside powder. Note that during 600 hrs of reaction time, no systematic variation of the surface
366 area for powder reacted at $5 < \text{pH} < 10$ in bacteria-free solutions was observed (Golubev and Pokrovsky,
367 2006).

368 Experiments were performed in series at constant flow rate between 0.018 and 0.022 mL/min. This
369 corresponded to a mechanical steady-state achievement (x 5 reactor volume renewal) after 4 to 5 days. At the
370 beginning of each series, a quantity of fresh diopside powder was added to the reactor system. For each
371 experimental series, a sterile bacteria-free 0.1 M NaCl with relevant buffer (10 mM NaMES (2-
372 morpholinoethanesulfonic acid) or NaHCO₃) was first prepared and injected into the reactor until a steady-
373 state outlet fluid composition was attained (typically 2 weeks, D1 series). Once steady state was attained, live
374 bacteria (0.54 g_{wet}/L) with or without nutrients were added to this inlet solution (D2 series). The next series
375 comprised higher concentration of live bacteria in the inlet fluid (3.85 g_{wet}/L). The 2nd and 3rd series lasted
376 7-10 days each. After that, the inlet solution was replaced by fresh sterile bacteria-free fluid; this experiment,
377 which lasted > 3 weeks, was destined to assess the recovery of the mineral reactivity and to test the
378 consequences of passivation of mineral surface by a bacterial biofilm.

379 The inlet solutions were composed of 0.1 M NaCl and 0.01 M NaMES (D1 and D2 series) and 0.1 M
380 NaCl with 0.01 M NaHCO₃ (D3 and D4 series). The 1:10 diluted Aldrich nutrient broth (0.1 g/L glucose, 1.5
381 g/L peptone, 0.6 g/L NaCl and 0.3 g/L yeast extract) was added to selected live bacteria experiments. These
382 were compared to live bacteria experiments performed without nutrients. Overall, the experiments conducted
383 in this study can be divided into three main categories: 1) bacteria- and nutrient-free, 2) live bacteria in
384 nutrient-free media, and 3) live bacteria in 10% growth media.

385 All outlet sample fluids were additionally filtered through 0.45 µm Millipore acetate cellulose filters
386 and acidified with ultrapure 2% HNO₃ before chemical analysis. The inlet fluids were routinely analyzed at
387 the beginning, in the middle and at the end of each experiment and were filtered and processed using exactly
388 the same protocol as the outlet fluids.

389 Mechanical steady-state was achieved after 24 h of reaction. For each steady-state condition,
390 minimum 4 independent measurements of Mg, Ca and Si concentrations, bacterial optical density, pH and
391 flow rate were performed (reproducibility of ± 10%) and used for calculating the dissolution rate. The cell
392 count (CFU) on nutrient agar plates was performed at the beginning, in the middle and at the end of each
393 experimental run and did not vary significantly throughout all experiments.

394

395 **Batch experiments on diopside dissolution in the presence of fungus**

396 The aim of these experiments was to compare, under identical solution conditions, the Ca, Mg and Si
397 release rate from diopside placed in contact with dead and live fungus cultures. The batch reactors used to
398 study diopside–fungus interaction consisted of sterile 250 mL polypropylene culture flasks with vented caps
399 (Biosilico). All manipulations were conducted in a sterile laminar hood box (class 100). For experiments, 1.3
400 g of sterilized 100-200 µm diopside were placed in 250 mL sterile solution. We conducted six experiments in
401 duplicates, four involving live cultures, with and without nutrient solution, and two with dead (autoclaved)
402 biomass (in nutrient-free 0.1 M NaCl).

403 The reactors were inoculated with 4.2-5.6 g_{wet}/L of fresh *Chaetomium brasiliense* culture or the
404 equivalent amount of dead biomass and placed on rotative shaker (120 rpm) at 25 ± 1°C for 19 days. Sterile
405 controls were routinely run both for nutrient media and 0.1 M NaCl solutions and did not demonstrate any
406 fungal contamination. Periodically, 10 mL aliquots of homogeneous mineral suspension + fungus were
407 collected using sterile serological pipettes and transferred in polystyrene vials for Ca, Mg, Si, pH and cell
408 biomass measurements. The mineral/fluid ratio remained constant during experiments and the concentration
409 of fungus was not affected by the sampling. Calcium, Mg and Si concentrations were analyzed in 0.45 µm
410 filtrates and pH and cell biomass were measured in unfiltered samples.

411

412 **Analyses**

413 All input and output solutions were analyzed for Mg, Ca, Si, optical density and pH as a function of time.
414 NIST buffers (pH = 4.008, 6.865, and 9.180 at 25°C) were used for calibration of a combination pH-
415 electrode (Schott Geräte H62). Magnesium and Ca concentrations were measured by flame atomic

416 absorption spectroscopy with an uncertainty of 1 and 2 % and a detection limit of 0.1 and 0.2 μM ,
417 respectively. Total silica concentration was determined by a Technicon automatic analyzer using the
418 molybdate blue method with an uncertainty of 2% and a detection limit of 0.3 μM . The concentration of
419 soluble organic exometabolites of bacteria and fungi was measured as total dissolved organic carbon (DOC)
420 using a TOC Shimadzu VSCN analyzer with an uncertainty of 5% and a detection limit of 0.1 $\text{mg C}_{\text{org}} \text{L}^{-1}$.
421 All experiments were performed at far from equilibrium conditions with respect to diopside as calculated via
422 vMinteq program¹⁰⁰ with relevant solubility parameters¹⁰¹.

423 **Microscopic observations**

424 A detailed AFM study using a biological instrument (JPK NanoWizard) allowed in-situ high-
425 resolution characterization of the status of diopside surfaces in the presence of live bacteria with and without
426 nutrients. Diopside cleavage planes were obtained by cleaving optically transparent crystals 5-10 mm in size
427 in a laminar hood box (A100). Fresh cleavage surfaces were sterilized by alcohol and fixed within petri
428 dishes for imaging with the AFM. For long-term (> 5 h) exposure, diopside cleavages were reacted under
429 sterile conditions with 1 $\text{g}_{\text{wet}}/\text{L}$ of bacterial biomass in separate petri dishes. The petri dishes were mounted
430 into the AFM for in-situ inspection of the diopside surfaces directly immersed within the bacteria containing
431 medium, removed from the microscope for further storage, and re-investigated with the microscope
432 whenever appropriate. Depending on the specific aim of the scanning process (attempt of potentially imaging
433 all adhering matter on the surface vs. attempt of removing matter adhering to the surface), images were
434 acquired with both intermittent-contact mode and contact mode using uncoated Si-cantilevers with integrated
435 tips.

436 The diopside grains reacted with fungus were examined by Scanning Electron Microscopy (SEM).
437 Prior to characterization by SEM, samples were centrifuged (3000 g, 30 min) and the organic matter was
438 removed from the solid phase by rinsing them in nutrient-free sterile 0.1 M NaCl solution. The remaining
439 solids were rinsed three times with MilliQ water and freeze-dried at -60 °C. They were observed after carbon
440 film coated on the sample surface with a JEOL JSM 6360LV SEM coupled with a SDD PGT Sahara EDS
441 analyzer operating at 30 kV.

442

443 **DATA AVAILABILITY**

444 Supplementary material is available. All measured dissolution rates are presented in Tables 1 and 2. Other
445 relevant data are also available from the corresponding author of this paper upon a reasonable request.

446

447 **REFERENCES**

- 448 1. Berner, R. A. Weathering, plants and the long-term carbon cycle. *Geochim. Cosmochim. Acta*, **56**, 3225-
449 3231 (1992).
- 450 2. Dupré, B., Dessert, C., Oliva, P., Goddérís, Y., Viers, J., Francois, L., Millot, R. & Gaillardet, J. Rivers,
451 chemical weathering and Earth's climate. *Compte Rendus. Geoscience* **335**, 1141-1160 (2003).
- 452 3. Landeweert, R., Hoffland, E., Finlay, R. D., Kuyper, T. W. & van Breemen, N. Linking plants to rocks:
453 ectomycorrhizal fungi mobilize nutrients from minerals. *Trends Ecol. Evol.* **16**, 248–254 (2001).
- 454 4. Hutchens, E., Valsami-Jones, E., McEldowney, S., Gaze, W. & McLean, J. The role of heterotrophic
455 bacteria in feldspar dissolution — an experimental approach. *Mining Magazine* **67**, 1157–1170 (2003).
- 456 5. Gadd, G. M. Geomycology: biogeochemical transformations of rocks, minerals, metals and radionuclides
457 by fungi, bioweathering and bioremediation. *Mycol. Res.* **111**, 3–49 (2007).
- 458 6. Olsen, A. A. & Rimstidt, D.J. Oxalate-promoted forsterite dissolution at low pH. *Geochim. Cosmochim.*
459 *Acta* **72**, 1758-1766 (2008).

- 460 7. Hutchens, E. Microbial selectivity on mineral surfaces: possible implications for weathering processes.
461 *Fungal Biology Rev.* **23**, 115–121 (2009).
- 462 8. Li, Z. B., Lu, X. C., Teng, H. H., Chen, Y., Zhao, L., Ji, J. F., Chen, J. & Liu L. W. Specificity of low
463 molecular weight organic acids on the release of elements from lizardite during fungal weathering.
464 *Geochim. Cosmochim. Acta* **256**, 20-34, doi : 10.1016/j.gca.2018.09.029 (2019).
- 465 9. Barker, W. W., Welch, S. A., & Banfield, J. F. Biogeochemical weathering of silicate minerals, in Banfield,
466 J.F. and Nealson K.H., editors, Geomicrobiology: Interactions Between Microbes and Minerals, *Rev.*
467 *Mineral.* **35**, 391-428 (1997).
- 468 10. Ullman, W. J., Kirchman, D. L., Welch, S. A. & Vandevivere, Ph. Laboratory evidence for microbially
469 mediated silicate mineral dissolution in nature. *Chem. Geol.* **132**, 11-17 (1996).
- 470 11. Welch, S. A., Barker, W. W. & Banfield, J. F. Microbial extracellular polysaccharides and plagioclase
471 dissolution. *Geochim. Cosmochim. Acta* **63**, 1405-1419 (1999).
- 472 12. Adamo, P. & Violante, P. Weathering of rocks and neogenesis of minerals associated with lichen activity.
473 *Applied Clay Science* **16**, 229-256 (2000).
- 474 13. Huang, W. H. & Keller, W. D. Dissolution of rock-forming minerals in organic acids: Simulated first stage
475 weathering of fresh mineral surfaces. *Amer. Mineral.* **55**, 2076-2094 (1970).
- 476 14. Huang, W. H. & Kiang, W. C. Laboratory dissolution of plagioclase in water and organic acids at room
477 temperature. *Amer. Mineral.* **57**, 1849-1859 (1972).
- 478 15. Manley, E. P. & Evans, L. J. Dissolution of feldspars by low-molecular-weight aliphatic and aromatic acids.
479 *Soil Science* **141**, 106-112 (1986).
- 480 16. Lundström, U. & Ohman, L.-O. Dissolution of feldspars in the presence of natural, organic solutes. *J. Soil*
481 *Sci.* **41**, 359-369 (1990).
- 482 17. Heyes, A. & Moore, T. R. The influence of dissolved organic carbon and anaerobic conditions on mineral
483 weathering. *Soil Science*, **154**, 226-236 (1992).
- 484 18. Ochs, M., Brunner, I., Stumm, W. & Cosovic, B. Effects of root exudates and humic substances on
485 weathering kinetics. *Water Air Soil Pollution* **68**, 213-229 (1993).
- 486 19. Drever, J. I. & Vance, G. F. Role of soil organic acids in mineral weathering processes. In: Pittman, E.D.,
487 Lewan, M.D. (Eds.), *Organic Acids in Geological Processes*. Springer Verlag, Berlin, pp. 138-161 (1994).
- 488 20. Stillings, L. L., Drever, J. I., Brantley, S.L., Sun, Y. & Oxburgh, R. Rates of feldspar dissolution at pH 3-7
489 in 0-8 mM oxalic acid. *Chem. Geol.* **132**, 79-90 (1996).
- 490 21. Drever, J. I. & Stillings, L. L. The role of organic acids in mineral weathering. *Colloids Surfaces A*, **120**,
491 167-181 (1997).
- 492 22. Barker, W. W., Welch, S. A., Chu, S. & Banfield, J. F. Experimental observations of the effects of bacteria
493 on aluminosilicate weathering. *Amer. Mineral.* **83**, 1551-1563 (1998).
- 494 23. Welch, S. A. & Ullman, W. J. The effect of microbial glucose metabolism on bytownite feldspar dissolution
495 rates between 5° and 35°C. *Geochim. Cosmochim. Acta* **63**, 3247-3259 (1999).
- 496 24. Bennett, P. C., Rogers, J. R. & Choi, W. J. Silicates, silicate weathering, and microbial ecology.
497 *Geomicrobiol. J.* **18**, 3-19 (2001).
- 498 25. Van Hees, P. A. W., Lundström, U. S. & Mörth, C.-M. Dissolution of microcline and labradorite in a forest
499 O horizon extract: the effect of naturally occurring organic acids. *Chem. Geol.* **189**, 199-211 (2002).

- 500 26. Neaman, A., Chorover, J. & Brantley, S. L. Effects of organic ligands on granite dissolution in batch
501 experiments at pH 6. *Amer. J. Sci.* **306**, 451-473 (2006).
- 502 27. Ganor, J., Reznik I.J. & Rosenberg, Y. O. Organics in Water-Rock Interactions: In: *Reviews in Mineralogy*
503 & *Geochemistry*, Thermodynamics and Kinetics of Water-Rock Interaction, eds: E.H. Oelkers and J.
504 Schott, **70**, 259-369 (2009).
- 505 28. Ahmed, E. & Holmström, S.J.M. Microbe-mineral interactions: The impact of surface attachment on
506 mineral weathering and element selectivity by microorganisms. *Chem. Geol.* **403**, 13-23 (2015).
- 507 29. Oelkers, E. H. & Schott, J. Does organic acid adsorption affect alkali-feldspar dissolution rates? *Chem.*
508 *Geol.* **151**, 235-245 (1998).
- 509 30. Kummert, R. & Stumm, W. The surface complexation of organic acids on hydrous Al₂O₃. *J. Colloid*
510 *Interface Sci.* **75**, 373-385 (1980).
- 511 31. Stumm, W. Reactivity at the mineral-water interface: dissolution and inhibition. *Colloids Surfaces A*, **120**,
512 143-166 (1997).
- 513 32. Schalscha, E. B., Appelt, M. & Schatz, A. Chelation as a weathering mechanism: 1. Effects of complexing
514 agents on the solubilisation of Fe from minerals and granodiorite. *Geochim. Cosmochim. Acta* **31**, 587-596
515 (1967).
- 516 33. White, A. F. & Yee, A. Aqueous oxidation-reduction kinetics associated with coupled electron-cation
517 transfer from iron containing silicates at 25°C. *Geochim. Cosmochim. Acta* **49**, 1263-1275 (1985).
- 518 34. Watteau, F. & Berthelin, J. Microbial dissolution of iron and aluminium from soil minerals: efficiency and
519 specificity of hydroxamate siderophores compared to aliphatic acids. *European J. Soil Biol.* **30**, 1-9 (1994).
- 520 35. Liermann, L. J., Kalinowski, B. E., Brantley, S. L. & Ferry, J. G. Role of bacterial siderophores in
521 dissolution of hornblende. *Geochim. Cosmochim. Acta* **64**, 587-602 (2000).
- 522 36. Santelli, C. M., Welch, S. A., Westrich, H. R. & Banfield, J. F. Fe oxidizing bacteria and the weathering of
523 Fe silicate minerals. *Chem. Geol.* **180**, 99-115 (2001).
- 524 37. Bonneville, S., Smits, M. M., Brown, A., Harrington, J., Leake, J. R., Brydson, R. & Benning, L. G. Plant-
525 driven fungal weathering: Early stages of mineral alteration at the nanometer scale. *Geology*, **37**, 615-618
526 (2009).
- 527 38. Gerrits, R., Pokharel, R., Breitenbach, R., Radnik, J., Feldmann, I., Schuessler, J. A., von Blankenburg, F.,
528 Gorbushina A. A. & Schott, J. How the rock-inhabiting fungus *K. petricola* A95 enhances olivine
529 dissolution through attachment. *Geochim. Cosmochim. Acta* **282**, 76-97,
530 <https://doi.org/10.1016/j.gca.2020.05.010> (2020).
- 531 39. Gerrits, R., Wirth, R., Schreiber, A., Feldmann, I., Knabe, N., Schott, J., Benning, L. G. & Gorbushina, A.
532 A. High-resolution imaging of fungal biofilm-induced olivine weathering. *Chem. Geol.* **559**, 119902
533 (2021).
- 534 40. Golubev, S. V., Bauer, A. & Pokrovsky, O. S. Effect of pH and organic ligands on the kinetics of smectite
535 dissolution at 25°C. *Geochim. Cosmochim. Acta*, **70**, 4436-4451 (2006).
- 536 41. Golubev, S. V. & Pokrovsky O. S. Experimental study of the effect of organic ligands on diopside
537 dissolution kinetics. *Chem. Geol.* **235**, 377-389 (2006).
- 538 42. Pokrovsky, O. S. & Schott, J. Kinetics and mechanism of dolomite dissolution in neutral to alkaline
539 solutions revisited. *Amer. J. Sci.* **301**, 597-626 (2001).
- 540 43. Pokrovsky, O. S., Schott, J. & Castillo, A. Kinetics of brucite dissolution at 25°C in the presence of organic
541 and inorganic ligands and divalent metals. *Geochim. Cosmochim. Acta* **69**, 905-918 (2005).

- 542 44. Pokrovsky, O. S., Golubev, S. V. & Jordan, G. Effect of organic and inorganic ligands on calcite and
543 magnesite dissolution rates at 60°C and 30 atm pCO₂. *Chem. Geol.* **265**, 33-43 (2009).
- 544 45. Pokrovsky, O. S., Shirokova, L. S., Bénézech, P., Schott, J. & Golubev, S. V. Effect of organic ligands and
545 heterotrophic bacteria on wollastonite dissolution kinetics. *Amer. J. Sci.* **309**, 731-772 (2009).
- 546 46. Jordan, G., Pokrovsky, O. S., Guichet, X. & Schmah, W. W. Organic and inorganic ligand effects on
547 magnesite dissolution at 100°C and pH = 5 to 10. *Chem. Geol.* **242**, 484-496 (2007).
- 548 47. Oelkers, E. H., Golubev, S. V., Pokrovsky, O. S. & Benezeth, P. Do organic ligands effect calcite
549 dissolution rates? *Geochim. Cosmochim. Acta* **75**, 1799-1813 (2011).
- 550 48. Stockmann, G. J., Shirokova, L. S., Pokrovsky, O. S., Bénézech, P., Bovet, N., Gislason, S. R. & Oelkers,
551 E.H. Does the presence of heterotrophic bacteria *Pseudomonas reactans* affect basaltic glass dissolution
552 rates? *Chem. Geol.* **296-297**, 1-18 (2012).
- 553 49. Shirokova, L. S., Pokrovsky, O. S., Bénézech, P., Gérard, E., Ménez, B. & Alfredsson, H. A. Experimental
554 study of the effect of heterotrophic bacterium (*Pseudomonas reactans*) on olivine dissolution kinetics in
555 the context of CO₂ storage in basalts. *Geochim. Cosmochim. Acta* **80**, 30-50 (2012).
- 556 50. Webley, D. M., Duff, R. B. & Mitchell W.A. Plate method for studying the breakdown of synthetic and
557 natural silicates by soil bacteria. *Nature*, **188**, 766-767 (1960).
- 558 51. Duff R. B., Webley D. M. & Scott R. O. Solubilization of minerals and related materials by 2-ketogluconic
559 acid-producing bacteria. *Soil Sci.* **95**, 105-114 (1962)
- 560 52. Aouad, G., Crovisier, J.-L., Geoffroy, V. A., Meyer, J.-M. & Stille, P. Microbially-mediated glass
561 dissolution and sorption of metals by *Pseudomonas aeruginosa* cells and biofilm. *J. Haz. Materials* **B136**,
562 889-895 (2006).
- 563 53. Brantley, S. L. & Chen, Y. Chemical weathering rates of pyroxenes and amphiboles. *Reviews in Mineralogy*
564 **31**, 119-172 (1995).
- 565 54. Schott, J., Pokrovsky, O. S. & Oelkers, E. H. The link between mineral dissolution/precipitation kinetics
566 and solution chemistry. *Rev. Mineral. Geochem.*, Thermodynamics and Kinetics of Water-Rock Interaction,
567 eds: E.H. Oelkers and J. Schott, **70**, 207-258 (2009).
- 568 55. Knauss, K. G., Nguyen, S. N. & Weed, H. C. Diopside dissolution kinetics as a function of pH, CO₂,
569 temperature, and time. *Geochim. Cosmochim. Acta* **57**, 285-294 (1993).
- 570 56. Golubev, S. V., Pokrovsky, O. S. & Schott, J. Experimental determination of the effect of dissolved CO₂
571 on the dissolution kinetics of Mg and Ca silicates at 25° C. *Chem. Geol.* **217**, 227-238 (2005).
- 572 57. Van der Aa, B. C. & Dufrene, Y. F. In situ characterization of bacteria extracellular polymeric substances
573 by AFM. *Colloid Surfaces B: Biointerfaces* **23**, 173-182 (2002).
- 574 58. Beech, I. B., Smith, J. R., Steele, A. A., Penegar, I. & Campbell, S. A. The use of atomic force microscopy
575 for studying interactions of bacterial biofilms with surfaces. *Colloid Surfaces B: Biointerfaces* **23**, 231-247
576 (2002).
- 577 59. Chen, J., Blume, H. P. & Beyer, L. Weathering of rocks induced by lichen colonization - a review. *Catena*
578 **39**, 121-146 (2000).
- 579 60. Buss, H. L., Luttge, A. & Brantley, S. L. Etch pit formation on iron silicate surfaces during siderophore-
580 promoted dissolution. *Chem. Geol.* **240**, 326-342 (2007).
- 581 61. Uroz, S., Calvaruso, C., Turpault, M.-P. & Frey-Klett, P. Mineral weathering by bacteria: ecology, actors
582 and mechanisms. *Trends Microbiol.* **17**(8), 378-387 (2009).

- 583 62. Vandevivere, P., Welch, S. A., Ullman, W. J. & Kirchman, D. L. Enhanced dissolution of silicate minerals
584 by bacteria at near-neutral pH. *Microbial Ecol.* **27**, 241-251 (1994).
- 585 63. Welch, S. A. & Vandevivere, P. Effect of microbial and other naturally occurring polymers on mineral
586 dissolution. *Geomicrobiol. J.* **12**, 227-238 (1994).
- 587 64. Roberts, J. A. Inhibition and enhancement of microbial surface colonization: the role of silicate
588 composition. *Chem. Geol.* **212**, 313-327 (2004).
- 589 65. Balogh-Brunstad, Z., Keller, C. K., Dickinson, J. T., Stevens, F., Li, C. Y. & Bormann, B. T. Biotite
590 weathering and nutrient uptake by ectomycorrhizal fungus, *Suillus tomentosus*, in liquid-culture
591 experiments. *Geochim. Cosmochim. Acta* **72**, 2601-2618 (2008).
- 592 66. Bundeleva, I. A., Menez, B., Auge, T., Bodenan, F., Recham, N. & Guyot F. Effect of cyanobacteria
593 *Synechococcus* PCC 7942 on carbonation kinetics of olivine at 20 degrees C. *Minerals Engineering* **59**, 2-
594 11, DOI: 10.1016/j.mineng.2014.01.019 (2014).
- 595 67. Tourney J. & Ngwenya B. T. The role of bacterial extracellular polymeric substances in geomicrobiology.
596 *Chem. Geol.* **386**, 115-132 (2014).
- 597 68. Oelkers, E. H., Benning, L. G., Lutz, S., Mavromatis, V., Pearce, C. R. & Plumper, O. The efficient long-
598 term inhibition of forsterite dissolution by common soil bacteria and fungi at Earth surface conditions.
599 *Geochim. Cosmochim. Acta* **168**, 222-235. <https://doi.org/10.1016/j.gca.2015.06.004> (2015).
- 600 69. Garcia, B., Lemelle, L., Rose-Koga, E., Perriat, P., Basset, R., Gillet, P. & Albarede F. An experimental
601 model approach of biologically-assisted silicate dissolution with olivine and *Escherichia coli* - Impact on
602 chemical weathering of mafic rocks and atmospheric CO₂ drawdown. *Appl. Geochem.* **31**, 216-227 (2013).
- 603 70. Pokharel, R., Gerrits, R., Schuessler, J. A. & von Blankenburg, F. Mechanisms of olivine dissolution by
604 rock-inhabiting fungi explored using magnesium stable isotopes. *Chem. Geol.* **525**, 18-27 (2019).
- 605 71. Burford, E.P., Fomina, M. & Gadd, G. M. Fungal involvement in bioweathering and biotransformation of
606 rocks and minerals. *Mineral. Magazine* **67**(6), 1127-1155, doi: 10.1180/0026461036760154 (2003).
- 607 72. Wu, L., Jacobson, A. D., Chen, H.-C. & Hausner, M. Characterization of elemental release during microbe-
608 basalt interactions at T = 28°C. *Geochim. Cosmochim. Acta* **71**, 2224-2239 (2007).
- 609 73. Wu, L. L., Jacobson, A. D., Hausner, M. Characterization of elemental release during microbe-granite
610 interactions at T=28 degrees C. *Geochim. Cosmochim. Acta* **72**(4), 1076-1095, doi:
611 10.1016/j.gca.2007.11.025 (2008).
- 612 74. Hausrath, E. M., Neman, A. & Bratnley, S. L. Elemental release rates from dissolving basalt and granite
613 with and without organic ligands. *Amer. J. Sci.* **309**, 633-660 (2009).
- 614 75. Etesami, H., Emami, S. & Alikhani, H. Potassium solubilizing bacteria (KSB): Mechanisms, promotion
615 of plant growth, and future prospects - a review. *J. Soil Sci. Plant Nutr.* **17**(4), 897-911 (2017).
- 616 76. Daval, D. Carbon dioxide sequestration through [silicate](#) degradation and carbon mineralisation: promises
617 and uncertainties. *NPJ Mat. Degradation* **2**(1) Art No 11 (2018).
- 618 77. Voelz, J. L., Johnson, N. W. & Chun, C. L. Quantitative dissolution of environmentally accessible iron
619 residing in iron-rich minerals: A review. *ACS Earth Space Chem.* **3**(8), 1371-1392 (2019).
- 620 78. David, S. R. & Geoffroy, V. A. A review of asbestos bioweathering by siderophore-producing
621 *Pseudomonas*: A potential strategy of bioremediation. *Microorganisms* **8**(12), Art No 1870 (2020).
- 622 79. Fomina, M. & Skorochod, I. Microbial interaction with clay minerals and its environmental and
623 biotechnological implications. *Minerals* **10**(10), Art No 861 (2020).

- 624 80. Lee, J.-U. & Fein, J.B. Experimental study of the effects of *Bacillus subtilis* on gibbsite dissolution rates
625 under near-neutral pH and nutrient-poor conditions. *Chem. Geol.* **166**, 193–202 (2000).
- 626 81. Davis, K. J., Nealson, K. H., & Lüttge, A. Calcite and dolomite dissolution rates in the context of microbe-
627 mineral surface interactions. *Geobiology* **5**, 191-205 (2007).
- 628 82. Lüttge, A. & Conrad, P. G. Direct observation of microbial inhibition of calcite dissolution. *Appl. Environ.*
629 *Microbiol.* **70**, 1627-1632 (2004).
- 630 83. Bonneville, S., Morgan D. J., Schmalenberger, A., Bray, A., Brown, A., Banwart, S. A. & Benning L. G.
631 Tree-mycorrhiza symbiosis accelerate mineral weathering: Evidences from nanometer-scale elemental
632 fluxes at the hypna-mineral interface. *Geochim. Cosmochim. Acta* **75**(22), 6988-7005 (2011).
- 633 84. Hue, N. V., Craddock, G. R. & Adams, F. Effect of organic acids on aluminum toxicity in subsoils. *Soil*
634 *Sci. Soc. Amer. J.* **50**, 28-34 (1986).
- 635 85. Hongve, D., Van Hees, P. A. W. & Lundstrom, U. S. Dissolved components in precipitation water
636 percolated through forest litter. *European J. Soil Sci.* **51**, 667-677 (2000).
- 637 86. Oelkers, E. H. & Gislason, S. R. The mechanism, rates and consequences of basaltic glass dissolution: I.
638 An experimental study of the dissolution rates of basaltic glass as a function of aqueous Al, Si and oxalic
639 acid concentration at 25°C and pH = 3 and 11. *Geochim. Cosmochim. Acta* **65**, 3671-3681 (2001).
- 640 87. Gislason, S. R., Arnorsson, S. & Armannsson, H. Chemical weathering of basalt in SW Iceland: effects of
641 runoff, age of rocks and vegetative/glacial cover. *Amer. J. Sci.* **296**, 837-907 (1996).
- 642 88. Pokrovsky, O. S., Schott, J., Kudryavtzev D. I. & Dupré B. Basalt weathering in Central Siberia under
643 permafrost conditions. *Geochim. Cosmochim. Acta* **69**(24), 5659-5680 (2005).
- 644 89. Dessert, C., Gaillardet, J., Dupré, B., Schott, J. & Pokrovsky, O.S. Fluxes of high- versus low-temperature
645 water-rock interactions in aerial volcanic areas: the example of the Kamchatka Peninsula, Russia.
646 *Geochim. Cosmochim. Acta* **73**, 148–169 (2009).
- 647 90. Berner, E. K. & Berner, R. A. Global environment: Water, Air, and Geochemical Cycles. Prentice Hall,
648 New Jersey (1996).
- 649 91. Drever, J. I. The effect of land plants on weathering rates of silicate minerals. *Geochim. Cosmochim. Acta*
650 **58**, 2325-2332 (1994).
- 651 92. White, A. F., Bullen, T. D., Davison, V. V., Schulz, M. S. & Clow, D. W. The role of disseminated
652 calcite in the chemical weathering of granitoid rocks. *Geochim Cosmochim Acta* **63**, 1939–1953 (1999).
- 653 93. White, A. F., Schulz, M. S., Lowenstern, J. B., Vivit, D. V., Bullen, T.D. The ubiquitous nature of
654 accessory calcite in granitoid rocks: Implications for weathering, solute evolution and petrogenesis.
655 *Geochim Cosmochim Acta* **69**, 1455–1471 (2005).
- 656 94. Goddérís, Y., François, L. M., Probst, A., Schott, J., Moncoulon, D., Labat, D. & Viville, D. Modelling
657 weathering processes at the catchment scale: The WITCH numerical model. *Geochim. Cosmochim. Acta*,
658 **70**, 1128-1147 (2006).
- 659 95. Schott, J., Pokrovsky, O. S., Spalla, O., Devreux, F., Gloter, A. & Mielczarski, J. A. Formation, growth and
660 transformation of leached layers during silicate minerals dissolution: The example of wollastonite.
661 *Geochim. Cosmochim. Acta*, **98**, 259–281 (2012).
- 662 96. Sverdrup, H. Chemical weathering of soil minerals and the role of biological processes. *Fungal Biol. Rev.*
663 **23**, 94-100 (2009).
- 664 97. Goddérís, Y., Schott, J. & Brantley, S. L. Reactive transport models of weathering. *Elements* **15**(2), 103-
665 106, DOI: 10.2138/gselements.15.2.103 (2019).
- 666 98. Maher, K. & Mayer, K. U. Tracking diverse minerals, hungry organisms, and dangerous contaminants using
667 reactive transport models. *Elements* **15**(2), 81-86, DOI: 10.2138/gselements.15.2.81 (2019).

668 99. Abdel-Azeem, A. Taxonomy and Biodiversity of the Genus Chaetomium in Different Habitats. In book: A.
669 M. Abdel-Azeem (ed.), Fungal Biology, Recent Developments on Genus Chaetomium (pp. 3-77).
670 Publisher: Springer Nature Switzerland AG https://doi.org/10.1007/978-3-030-31612-9_1 (2020).

671 100. Gustafsson, J. Visual MINTEQ Ver. 3.1. <<http://vminteq.lwr.kth.se>> (assessed 8.05.2021) (2014)

672 101. Dixit, S. & Carroll, S. A. Effect of solution saturation state and temperature on diopside dissolution.
673 *Geochim. Trans.* **8**, 3, doi:10.1186/1467-4866-8-3 (2007).

674 **AUTHOR CONTRIBUTIONS**

675 O.S.P. developed the concept of the study. L.S.S., S.A.Z. and O.S.P. performed dissolution experiments. G.J.
676 performed AFM study. P.B. participated in laboratory experiments and SEM study. O.S.P. wrote the paper,
677 with input from L.S.S., P.B., G.J. and S.A.Z. All the co-authors discussed the final version of the paper.

678

679 **COMPETING INTERESTS**

680 The authors declare no competing interests.

681

682 **ADDITIONAL INFORMATION**

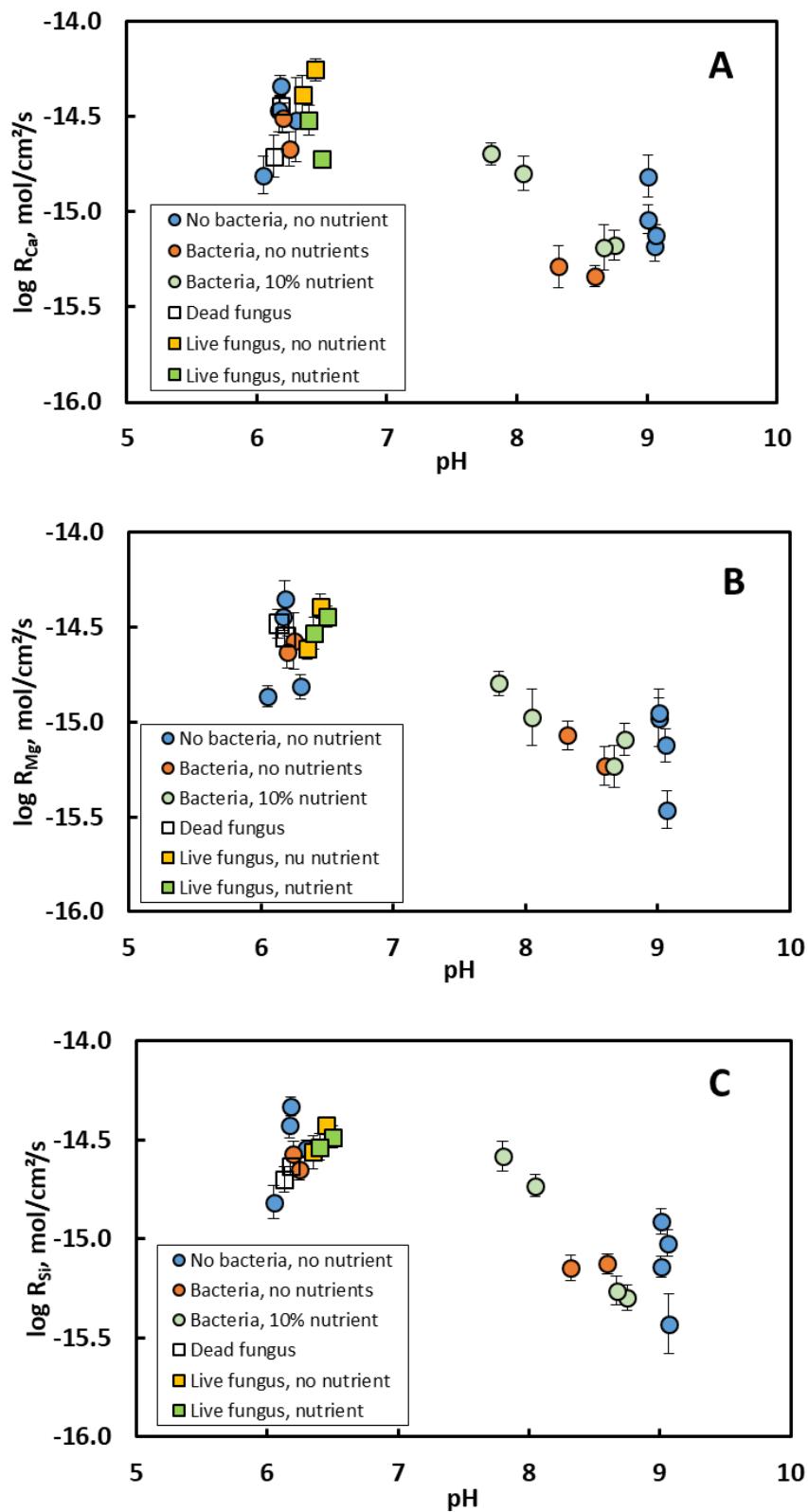
683 **Supplementary information** The online version contains supplementary material available at
684 <https://doi.org/XXXXXX>.

685 **Correspondence** and requests for materials should be addressed to O.S.P.

686 **Reprints and permission information** is available at <http://www.nature.com/reprints>

687 **Publisher's note** Springer Nature remains neutral with regard to jurisdictional claims in published maps and
688 institutional affiliations.

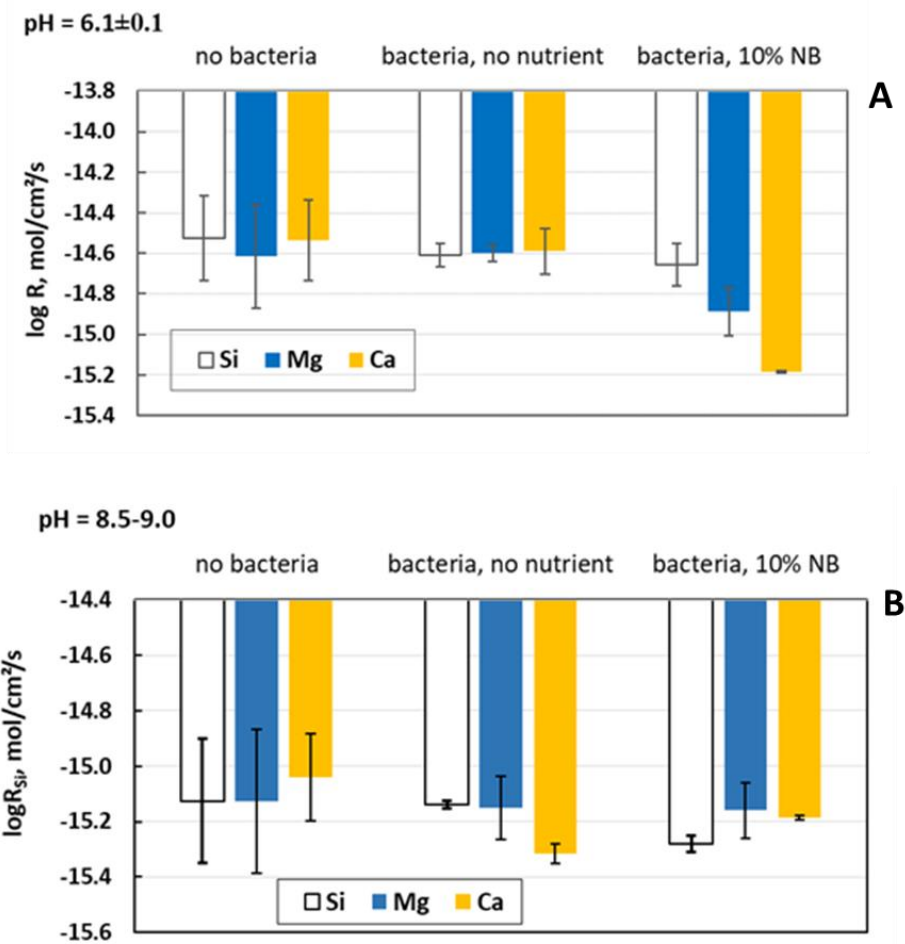
689



690

691

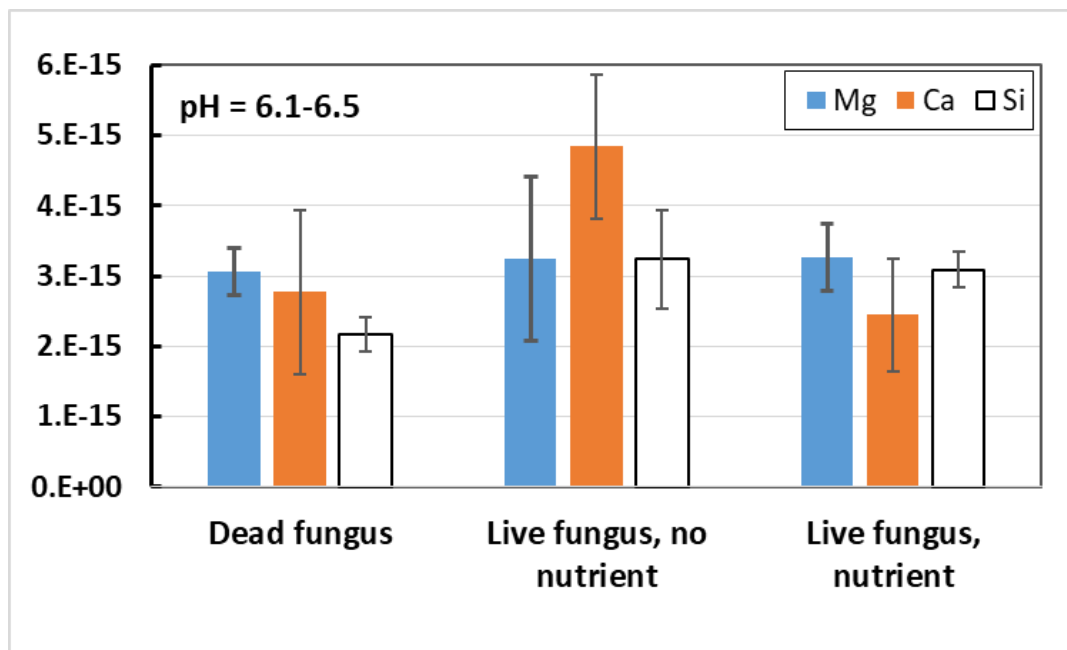
692 **Fig. 1.** Calcium (A), Mg (B) and Si (C) release rate from diopside measured in the mixed-flow reactor with
 693 and without bacteria and 10% nutrient or nutrient-free solution.



694

695

696 **Fig. 2.** Synthesis of obtained steady-state Ca, Mg and Si release rates (average ± s.d.) from diopside at pH 6
 697 (A) and 9 (B) with and without *Pseudomonas reactans* and in the presence or not of nutrients. The error bars
 698 represent average of 2 to 4 duplicates, each comprising 3 to 4 independent sampling at the steady state.



699

700

701

702 **Fig. 3.** Synthesis of obtained Ca, Mg and Si release rates (average \pm s.d., mol cm⁻² s⁻¹) from diopside at pH
 703 6.0-6.5 with and without *Chaetomium brasiliense* fungus (4.5-5.6g_{wet}/L) and in the presence or not of
 704 nutrients (1% Czapek medium). The error bars represent average of 2 reactors, each comprising 9 to 10
 705 independent sampling as a function of time over 19 days of exposure.

706

707

708

709

710

711

712

713

714

715

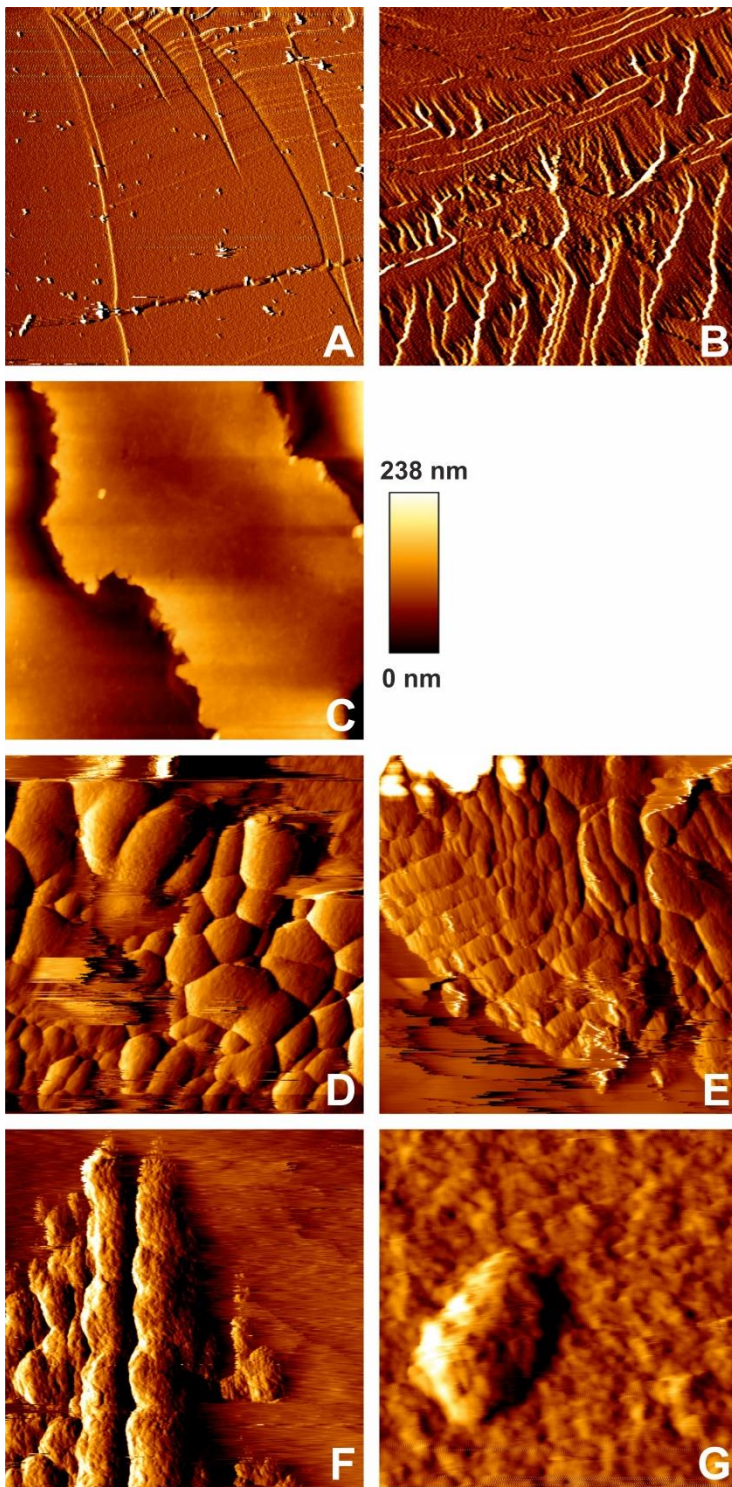
716

717

718

719

720



721

722 **Figure 4. A-C:** In-situ AFM images of diopside surfaces immersed within sterile electrolyte media for up to
 723 5 hours (**A:** 70 x 70 μm^2 , deflection mode; **B:** 20 x 20 μm^2 , deflection mode; **C:** 12 x 12 μm^2 , height mode -
 724 with the color scale spanning a total of 238 nm). **D-G:** In-situ AFM images of diopside surfaces immersed in
 725 nutrient media (**D:** 8.6 x 8.6 μm^2 , deflection mode; **E:** 10 x 10 μm^2 , deflection mode; **F:** 5.5 x 5.5 μm^2 ,
 726 deflection mode; **G:** 1.5 x 1.5 μm^2 , deflection mode).

727

728

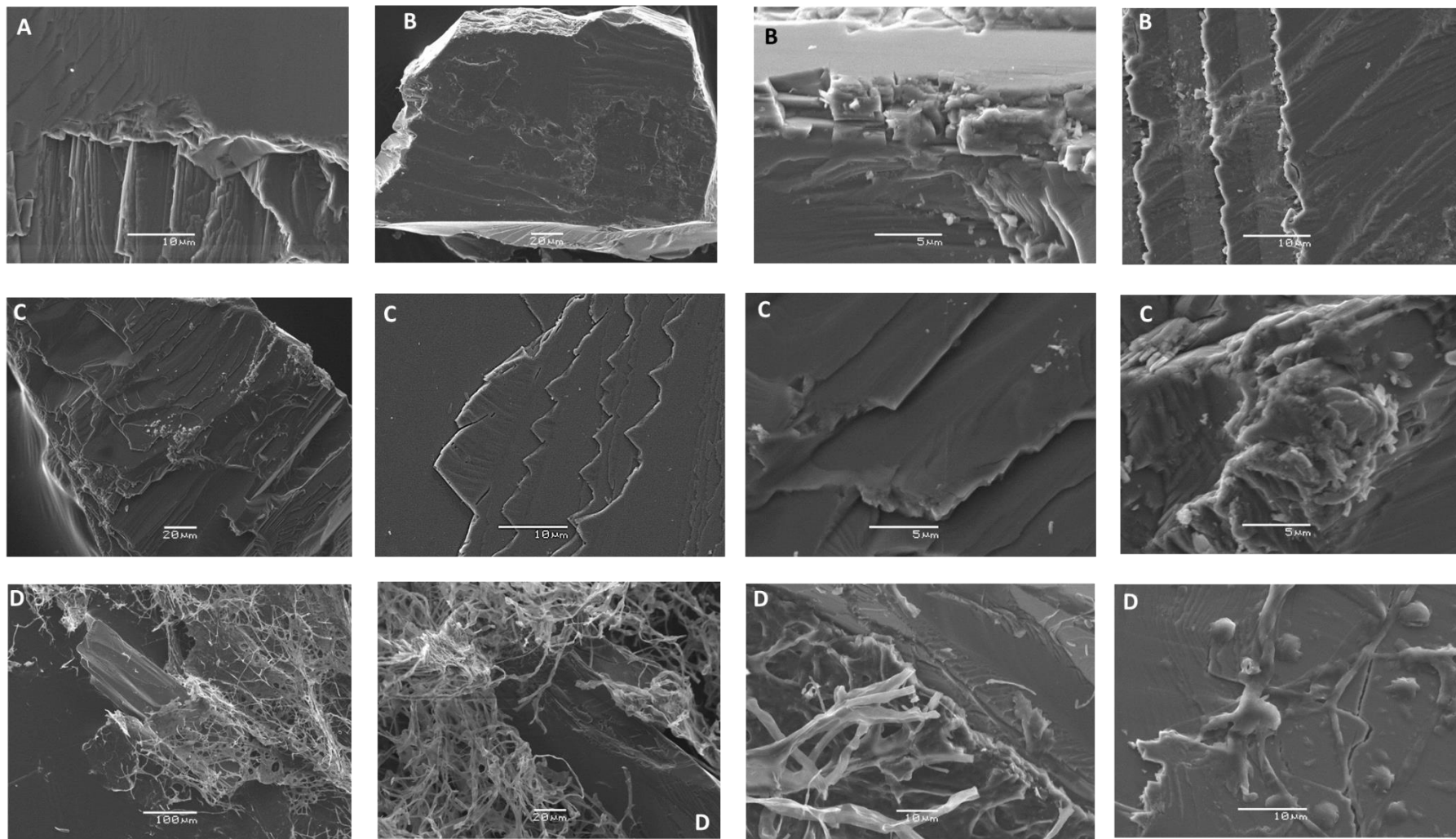


Figure 5. SEM images of reacted diopside surfaces in the sterile electrolyte (A), live fungus in 0.1 M NaCl (B, D) and 1% nutrient media (C, D).

Table 1. Results of Bacterial MFR experiment. R units are $\text{mol cm}^{-2} \text{s}^{-1}$.

Experiment	pH	$\log R_{\text{Ca}}$	$\log R_{\text{Mg}}$	$\log R_{\text{Si}}$
D1-1 0.1 M NaCl + 0.01 M MES, no bugs, no nutrients	6.18	-14.34±0.055	-14.35±0.10	-14.33±0.050
D2-1 0.1 M NaCl + 0.01 M MES, no bugs, no nutrients	6.17	-14.47±0.110	-14.44±0.075	-14.42±0.061
D2-4 0.1 M NaCl + 0.01 M MES, no bacteria, no nutrients	6.05	-14.81±0.10	-14.86±0.055	-14.81±0.085
D1-4 0.1 M NaCl + 0.01 M MES, no bacteria, no nutrients	6.30	-14.52±0.22	-14.81±0.065	-14.54±0.045
D3-4 0.1 M NaCl + 0.01 M NaHCO ₃ , no bacteria, no nutrients	9.01	-15.04±0.075	-14.98±0.15	-15.14±0.056
D3-1 0.1 M NaCl + 0.01 M NaHCO ₃ , no bugs, no nutrients	9.06	-15.18±0.078	-15.12±0.085	-15.02±0.065
D4-1 0.1 M NaCl + 0.01 M NaHCO ₃ , no bugs, no nutrients	9.07	-15.12±0.055	-15.46±0.10	-15.43±0.15
D4-4 0.1 M NaCl + 0.01 M NaHCO ₃ , no bacteria, no nutrients	9.01	-14.82±0.11	-14.95±0.075	-14.91±0.065
D1-2 0.1 M NaCl + 0.01 M MES, 0.54 g/l bacteria, no nutrients	6.25	-14.67±0.089	-14.57±0.15	-14.65±0.052
D1-3 0.1 M NaCl + 0.01 M MES, 3.85 g/l bacteria, no nutrients	6.20	-14.51±0.078	-14.63±0.082	-14.57±0.065
D3-2 0.1 M NaCl + 0.01 M NaHCO ₃ , 0.54 g/l bacteria, no nutrients	8.60	-15.34±0.055	-15.23±0.10	-15.13±0.05
D3-3 0.1 M NaCl + 0.01 M NaHCO ₃ , 3.85 g/l bacteria, no nutrients	8.32	-15.29±0.11	-15.07±0.075	-15.15±0.065
D2-2 0.1 M NaCl + 0.01 M MES, 0.54 g/l bacteria, 10% NB	7.80	-14.70±0.058	-14.80±0.065	-14.58±0.075
D2-3 0.1 M NaCl + 0.01 M MES, 3.85 g/l bacteria, 10% NB	8.05	-14.80±0.089	-14.97±0.15	-14.73±0.055
D4-2 0.1 M NaCl + 0.01 M NaHCO ₃ , 0.54 g/l bacteria, 10% NB	8.75	-15.18±0.078	-15.09±0.085	-15.30±0.065
D4-3 0.1 M NaCl + 0.01 M NaHCO ₃ , 3.85 g/l bacteria, 10% NB	8.67	-15.19±0.12	-15.23±0.11	-15.26±0.072

Table 2. Results of fungus batch experiments (0.1 M NaCl). R units are mol cm⁻² s⁻¹.

Experiment	pH	log R_{Mg}	log R_{Ca}	log R_{Si}
Dead biomass, 4.46 g/L	6.18	-14.55±0.10	-14.44±0.054	-14.63±0.051
Dead biomass, 4.95 g/L	6.13	-14.48±0.074	-14.71±0.11	-14.70±0.065
Live biomass, 4.83 g/L, no nutrient	6.35	-14.62±0.055	-14.39±0.10	-14.56±0.085
Live biomass, 5.1 g/L, no nutrient	6.45	-14.39±0.065	-14.25±0.058	-14.43±0.045
Live biomass, 5.6 g/L live, 1% nutrient	6.50	-14.44±0.055	-14.73±0.045	-14.49±0.054
Live biomass, 5.1 g/L, live, 1% nutrient	6.40	-14.53±0.085	-14.52±0.078	-14.54±0.067

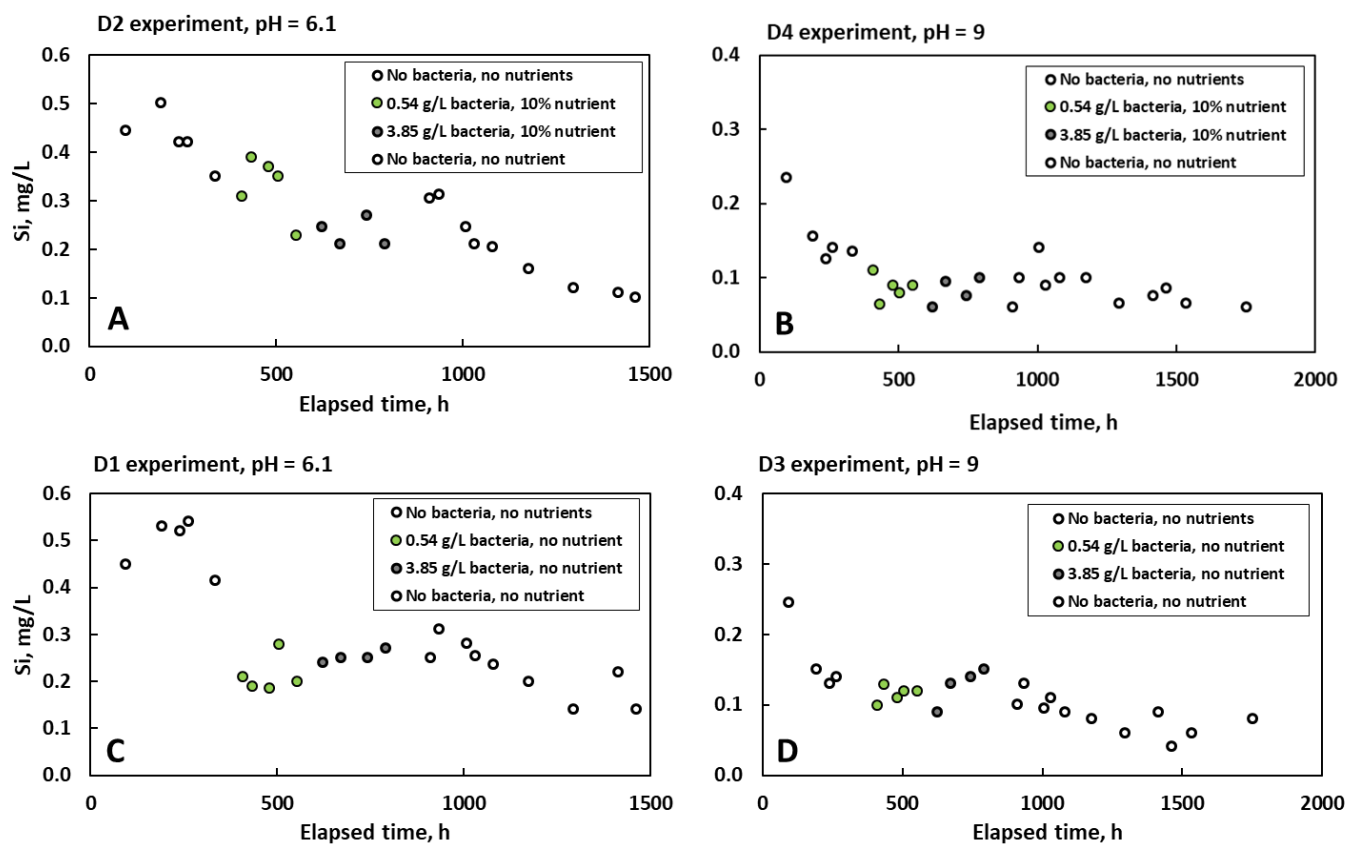


Fig. S1. Outlet Si concentration in the mixed-flow reactor at pH 6 (A) and 9 (B) in the sequence of nutrient-inlet solutions “bacteria-free 0.1 M NaCl → 0.54 g_{wet}/L bacteria, nutrient → 3.85 g_{wet}/L bacteria, nutrient → bacteria-free 0.1 M NaCl”. C and D: Outlet Si concentration in the mixed-flow reactor at pH 6 (C) and 9 (D) in the sequence of nutrient-free inlet solutions “bacteria-free 0.1 M NaCl → 0.54 g_{wet}/L bacteria, 0.1 M NaCl → 3.85 g_{wet}/L bacteria, 0.1 M NaCl → bacteria-free 0.1 M NaCl”.

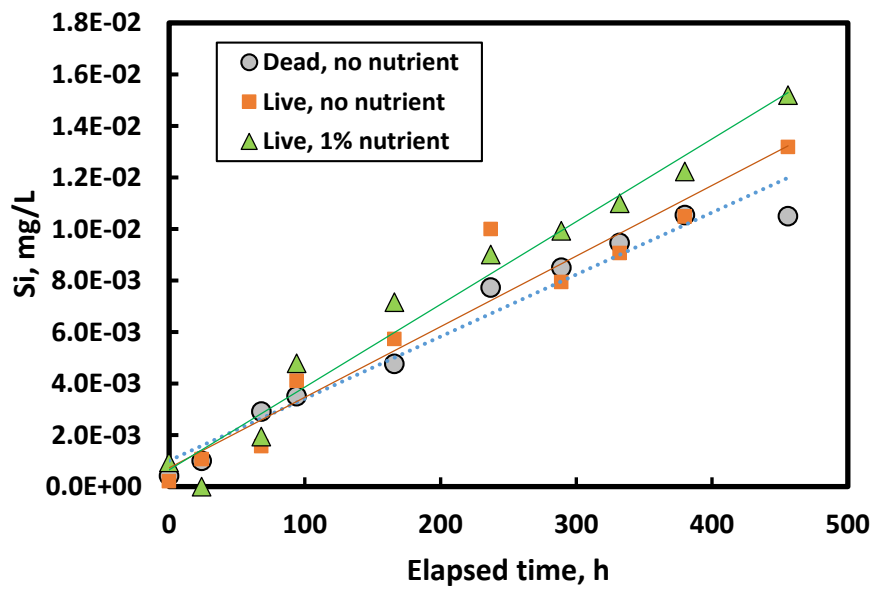


Fig. S2. Example of Si concentration evolution in batch reactor with dead, live without nutrient and live with 1% nutrients fungus (4.5, 4.2 and 5.6 g_{wet}/L , respectively).